MMTok: Multimodal Coverage Maximization for Efficient Inference of VLMs

Anonymous authors
Paper under double-blind review

Abstract

Vision-Language Models (VLMs) demonstrate impressive performance in understanding visual content with language instruction by converting visual inputs to vision tokens. However, redundancy in vision tokens results in the degenerated inference efficiency of VLMs. While many algorithms have been proposed to reduce the number of vision tokens, most of them apply only unimodal information (i.e., vision/text) for pruning and ignore the inherent multimodal property of vision-language tasks. Moreover, it lacks a generic criterion that can be applied to different modalities. To mitigate this limitation, in this work, we propose to leverage both vision and text tokens to select informative vision tokens by the coverage criterion. We first formulate the subset selection problem as a maximum coverage problem. Afterwards, a subset of vision tokens is optimized to cover the text tokens and the original set of vision tokens, simultaneously. The proposed method MMTok is extensively evaluated on benchmark datasets with different VLMs. The comparison illustrates that vision and text information are complementary, and combining multimodal information can surpass the unimodal baseline with a clear margin. Moreover, under the maximum coverage criterion on the POPE dataset, our method achieves a 1.87× speedup while maintaining 98.7% of the original performance on LLaVA-NeXT-13B. Furthermore, with only four vision tokens, 87.7% of the original performance is still preserved on LLaVA-1.5-7B. These results highlight the effectiveness of coverage in token selection.

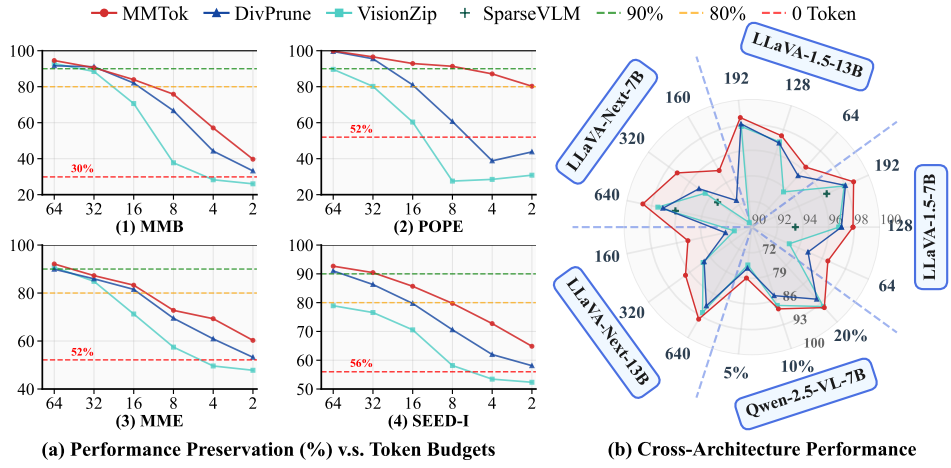

(a) Performance Preservation (%) v.s. Token Budgets (b) Cross-Architecture Performance

Figure 1: MMTok achieves better performance across multiple benchmarks.

1 Introduction

By converting the visual input to vision tokens, Vision-Language Models (VLMs) can leverage powerful Large Language Models (LLMs) to understand visual content as text (Liu et al., 2024b; Li et al., 2024b; Team et al., 2023). Unlike discrete text tokens, where the information is highly compressed, current vision encoders extract vision tokens directly from the original input patches,

which are redundant according to previous studies (Bolya et al., 2022; He et al., 2022) and their count can far exceed that of text tokens. For example, given "Describe the image" with less than 10 text tokens, $2,880$ vision tokens can be obtained from a single image in LLaVA-NeXT (Liu et al., 2024a).

Since LLMs are built on self-attention layers (Vaswani et al., 2017) that have a quadratic computational cost to the total number of tokens, the large volume of vision tokens can significantly challenge the inference efficiency of VLMs. To accelerate inference, many works (Shang et al., 2024; Yang et al., 2025a; Zhang et al., 2024) have been proposed to sample a subset of vision tokens for inference with LLMs without compromising performance. While some work adopts an additional training process (Yang et al., 2025a) to enable vision token selection, in this work, we will focus on the training-free paradigm to reduce optimization efforts. Our experiments also confirm that the proposed training-free method can even outperform baselines with fine-tuning.

Despite different architectures of VLMs (Team, 2024; Bai et al., 2025; Guo et al., 2025), the leading performance is from the one containing a separated vision encoder to obtain vision tokens (Bai et al., 2025). In that architecture, both vision tokens and text tokens are available for token selection before applying LLMs. However, most of the existing work relies on *unimodality* for pruning while the multimodal information has not been explored sufficiently (Zhang et al., 2024; Yang et al., 2025a; Alvar et al., 2025). For example, SparseVLM (Zhang et al., 2024) mainly considers text tokens from language instruction to guide the pruning of vision tokens, while VisionZip (Yang et al., 2025a) heavily depends on the `[CLS]` vision token to select informative vision tokens. By investigating vision-language tasks, we find that given the same image, the answers can be different due to user-specific text queries, while the same text instruction can be applied for different images, i.e., caption tasks. Therefore, a unimodal method is hard to capture sufficient information about target tasks, implying a suboptimal performance for token selection.

In order to leverage both vision and text information to obtain informative vision tokens, in this work, we propose a multimodal strategy for efficient inference. First, we formulate the token selection problem as a **maximum coverage problem**, which aims to cover the target tokens with a subset of source tokens. While the source tokens are vision-only, the target ones can come from either text or vision, respectively. Therefore, the framework can explicitly combine the information from different modalities. Then, we optimize the coverage problem by maximizing a submodular function defined on the similarity between target and source tokens. Although the original problem is NP-hard (Khuller et al., 1999), a simple greedy algorithm can observe an approximate solution that is not worse than $(1 - 1/e)$ of the optimal solution (Nemhauser et al., 1978). The main contributions of this work are summarized as follows.

- We introduce the maximum coverage problem for vision token selection. The problem can be formulated as maximizing a submodular function, which has an efficient algorithm to obtain a near-optimal solution with a theoretical guarantee.
- We apply the coverage criterion to cover both the text tokens and the entire set of vision tokens with a subset of selected vision tokens. The text-vision and vision-vision coverage explicitly help explore multimodal information for selection.
- Experiments are conducted on benchmark datasets with diverse VLMs. The superior performance of the proposed method demonstrates the effectiveness of the proposed coverage criterion for the subset selection of vision tokens. For example, the proposed MMTok can achieve overall best performance under different settings as illustrated in Figure 1 (b) and shows the potential to compress to an extremely small number of vision tokens as in Figure 1 (a).

2 Related Work

VLMs, such as LLaVA (Liu et al., 2023), InstructBLIP (Dai et al., 2023), and Qwen (Bai et al., 2025), have become a cornerstone for multimodal understanding by integrating large-scale vision encoders (e.g., CLIP-ViT (Radford et al., 2021b)) with pre-trained language models. These models achieve strong performance by representing images as sequences of visual tokens, but their inference cost grows quadratically with token count, highlighting the need for more efficient processing.

Many vision token selection methods have been proposed recently, but most of them rely only on unimodal information for pruning (Yang et al., 2025a; Shang et al., 2024; Chen et al., 2024a; Zhang et al., 2024; Alvar et al., 2025). For example, VisionZip (Yang et al., 2025a) and FastV (Chen et al.,

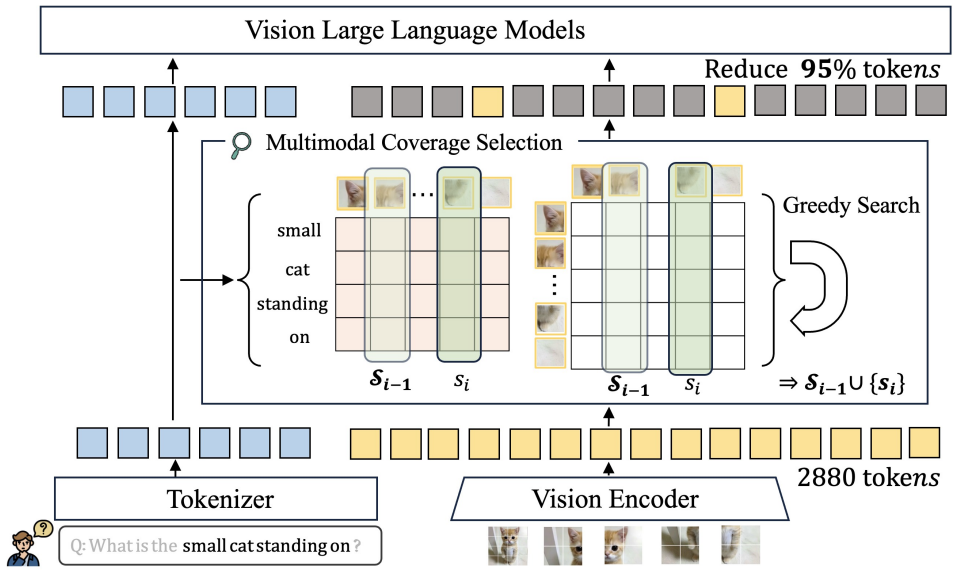

Figure 2: **Overview of MMTok framework.** Our method optimizes two maximum coverage problems simultaneously to leverage text-vision and vision-vision similarity for vision token selections.

2024a) prune tokens using pre-trained attention signals, either ranking by [CLS] token attention (VisionZip) or discarding low-attention vision tokens in deeper layers (FastV). Besides ranking, DivPrune (Alvar et al., 2025) uses a diversity-based criterion but only has vision tokens to maximize the intra-set diversity. These methods rely on vision information and may miss query-related semantics (Jain & Wallace, 2019; Wiegreffe & Pinter, 2019). SparseVLM (Zhang et al., 2024) instead uses text-to-vision attention for scoring, yet ignores the information from the whole image. To mitigate the gap between existing unimodal algorithms and target multimodal tasks, we propose a coverage-based criterion to leverage both vision and text information sufficiently to select vision tokens effectively.

3 The Proposed Method

To leverage the power of pre-trained models, many existing VLMs adopt a pre-trained vision encoder to extract vision tokens from images and then concatenate them with text tokens as input for the pre-trained LLMs. Although the simple architecture demonstrates promising performance, the inference efficiency can be challenging. Concretely, given an image, a pre-defined number of vision tokens will be obtained as $\{\mathbf{v}_1, \ldots, \mathbf{v}_n\}$. Even for a small 336×336 image, n is 576 with the ViT-L-336px from CLIP (Radford et al., 2021a), which is much larger than that of the text tokens from the text query (Liu et al., 2023). The large n will significantly slow down the inference of LLMs, which relies on the self-attention operations, and the complexity is quadratic to the total number of tokens.

To accelerate the inference of VLMs, we propose to select an informative subset of vision tokens $\{v_s\}_{s\in\mathcal{S}}$ to reduce the number of input tokens for LLM in VLM, where $\mathcal{N} = \{1, \ldots, n\}$, $\mathcal{S} \subseteq \mathcal{N}$, and $|\mathcal{S}| \ll n$. Figure 2 illustrates the framework of our method, and we will elaborate it as follows.

3.1 Vision Token Selection by Coverage Maximization

Unlike most of the existing work, we apply coverage as the main criterion for token selection. Given a similarity matrix $M \in \mathbb{R}^{m,n}$ defined between target tokens and source tokens, where m denotes the number of target tokens and n is the number of source tokens, a subset $\mathcal{S}$ will be selected to maximize the similarity between the target and selected tokens as

$$f(\mathcal{S}; M) = \frac{1}{m}\sum_{i=1}^{m} \max M_{i,\mathcal{S}}; \quad \mathcal{S}^* = \arg\max_{\mathcal{S}} f(\mathcal{S}; M) \tag{1}$$

a.k.a. covering the target tokens by an appropriate subset of source tokens. We first find that Eq. 1 is a popular submodular function (Leskovec et al., 2007).

Proposition 1. *(Leskovec et al., 2007) For all subsets $\mathcal{A} \subseteq \mathcal{B} \subseteq \mathcal{N}$ and $s \in \mathcal{N} \setminus \mathcal{B}$,*

$$f(\mathcal{A} \cup \{s\}) - f(\mathcal{A}) \geq f(\mathcal{B} \cup \{s\}) - f(\mathcal{B})$$

Maximizing submodular functions in general is NP-hard (Khuller et al., 1999), but a simple greedy algorithm can achieve a good approximation.

Proposition 2. *(Nemhauser et al., 1978) Let $\mathcal{S}$ denote the subset obtained by the greedy algorithm, then we have*

$$f(\mathcal{S}) \geq (1 - 1/e) \max_{\mathcal{A}:|\mathcal{A}|=|\mathcal{S}|} f(\mathcal{A})$$

We elaborate on how to apply the coverage function for token selections in the following subsections.

3.1.1 Maximum Text-Vision Coverage

First, we consider covering the semantics from text tokens with source vision tokens, which aims to find the vision tokens related to the text input (e.g., query). Let $\{\mathbf{t}_1, \ldots, \mathbf{t}_m\}$ denote the text tokens from the query. A similarity matrix between text and vision tokens can be obtained as

$$M^{tv}_{i,j} = \mathbf{t}_i^\top \mathbf{v}_j$$

where $M^{tv} \in \mathbb{R}^{m \times n}$ and $\forall i, j, \|\mathbf{t}_i\|_2 = \|\mathbf{v}_j\|_2 = 1$. To align the semantic similarity between text and vision, we adopt the vision tokens after the projection layer (i.e., those concatenated with text tokens as input for LLMs). After obtaining the appropriate similarity matrix, a subset of vision tokens can be selected to maximize the similarity between all text tokens and selected vision tokens for coverage as

$$\mathcal{S}' = \arg\max_{\mathcal{S}} f(\mathcal{S}; M^{tv})$$

According to Proposition 2, a greedy algorithm as summarized in Alg. 1 can approximate the optimal solution. It should be noted that the proposed Alg. 1 contains only simple operations (e.g., addition, matrix multiplication, etc.) and thus is efficient for implementation.

Algorithm 1 A Greedy Algorithm to Cover Text Input with Vision Tokens

Input: Similarity Matrix M^{tv}, k
Initialize $\mathcal{S} = \emptyset$
for $i = 1, \cdots, k$ **do**
  for $s \in \mathcal{N} \setminus \mathcal{S}$ **do**
    Compute $g(s) = f(\mathcal{S} \cup s; M^{tv})$
  end for
  Obtain $s_i = \arg\max_s g(s)$
  $\mathcal{S} = \mathcal{S} \cup s_i$
end for
return $\mathcal{S}$

Algorithm 2 MMToK: A Greedy Algorithm for Multimodal Coverage

Input: Similarity Matrices $M^{tv'}$, $M^{vv'}$, k
Initialize $\mathcal{S} = \emptyset$
for $i = 1, \cdots, k$ **do**
  for $s \in \mathcal{N} \setminus \mathcal{S}$ **do**
    Compute $g(s) = f(\mathcal{S} \cup s; M^{tv'}, M^{vv'})$
  end for
  Obtain $s_i = \arg\max_s g(s)$
  $\mathcal{S} = \mathcal{S} \cup s_i$
end for
return $\mathcal{S}$

3.1.2 Maximum Vision-Vision Coverage

Although text-vision coverage can explore vision information according to text, it may be insufficient due to vague text, e.g., "Please describe the image". Therefore, we propose to cover all vision information with a limited number of vision tokens. Concretely, a vision-vision similarity matrix can be generated as

$$M^{vv}_{i,j} = \mathbf{v}_i^{'\top} \mathbf{v}_j^{'}$$

where $M^{vv} \in \mathbb{R}^{n \times n}$. Unlike M^{tv} that adopts vision tokens after the projection layer to align with text tokens, those before projection are more appropriate to capture similarity between vision tokens without mixing text information. We have $\mathbf{v}'$ to distinguish it from the one after projection (i.e., $\mathbf{v}$).

Then, we can apply the greedy algorithm to select a subset of vision tokens to cover the main information implied by the whole set of vision tokens. Obviously, vision-vision coverage is complementary to text-vision coverage, which is also confirmed by our ablation study. The remaining challenge is to combine the two maximum coverage problems, which is described in the next subsection.

3.1.3 Maximum Multimodal Coverage

The maximum coverage problem can be applied to the original text and vision tokens simultaneously. However, M^{tv} and M^{vv} have different shapes and similarity measurements. Therefore, their values must be aligned before fusion. To calibrate the similarity between different modalities, the score for each row, i.e., that for target tokens, is first normalized by a softmax operation as

$$M^{tv'}_{i,j} = \frac{\exp(M^{tv}_{i,j}/\tau_t)}{\sum_{j=1}^{n}\exp(M^{tv}_{i,j}/\tau_t)}; \quad M^{vv'}_{i,j} = \frac{\exp(M^{vv}_{i,j}/\tau_v)}{\sum_{j=1}^{n}\exp(M^{vv}_{i,j}/\tau_v)}$$

where the softmax operation normalizes each row to a distribution over all vision tokens. τ_t and τ_v aim to further normalize the distribution shape for text-vision and vision-vision, respectively.

After calibration, the final objective for multimodal coverage can be written as

$$f(\mathcal{S}; M^{tv'}, M^{vv'}) = f(\mathcal{S}; M^{tv'}) + \alpha f(\mathcal{S}; M^{vv'}) \tag{2}$$

where α is used to weigh the importance of vision-vision coverage. Incorporating text-vision coverage with vision-vision coverage, the function in Eqn. 2 is still a submodular function as follows.

Corollary 1. *The sum of two submodular functions is a submodular function.*

Proof. It comes from the addition property of inequalities directly. □

With Corollary 1, we can apply a similar greedy algorithm to obtain the near-optimal solution for the multimodal scenario efficiently. The detailed algorithm is summarized in Alg. 2.

4 Experiments

To evaluate the performance of the proposed method, MMTok, we conduct experiments on diverse benchmark datasets and VLMs with different architectures. For a fair comparison, we conduct experiments on the datasets adopted in VisionZip (Yang et al., 2025a), which contains GQA (Hudson & Manning, 2019), MMBench (Liu et al., 2024c), MME (Fu et al., 2023), POPE (Li et al., 2023b), ScienceQA(IMG) (Lu et al., 2022), VQAv2-Test-Dev (Goyal et al., 2017), TextVQA (Singh et al., 2019), MMMU (Yue et al., 2024), and SeedBench (Li et al., 2023a). Meanwhile, five VLMs are applied for comparison, that is, LLaVA-1.5-7B (Liu et al., 2023), LLaVA-1.5-13B (Liu et al., 2023), LLaVA-NeXT-7B (Liu et al., 2024a), LLaVA-NeXT-13B (Liu et al., 2024a), and a recent model Qwen-2.5-VL-7B (Bai et al., 2025). Finally, we compare our method with state-of-the-art vision token pruning algorithms, including FastV (Chen et al., 2024a) (a vision-based method), SparseVLM (Zhang et al., 2024) (a language-based method), VisionZip (Yang et al., 2025a) (a [CLS]-importance-based method), and DivPrune (Alvar et al., 2025) (a diversity-based method). We also include a fine-tuning-based method, VisionZip🔥, in the comparison. We obtain the result of DivPrune through its official code, and that for other baselines is directly from (Yang et al., 2025a). Evaluation is implemented within the `Lmms-eval` framework (Li et al., 2024a) with the details elaborated as follows.

Implementation Details The proposed method relies on an appropriate similarity for coverage optimization. Since different layers may demonstrate different similarity measurements (Liu et al., 2023), we have the vision tokens before the projection layer to compute vision-vision similarity, while those after the projection layer are for text-vision coverage. It is because the latter layer aligns better with text. We find that our method is not sensitive to hyperparameters, as shown in the ablation study. Therefore, we fix $\tau_t = 0.02$, $\tau_v = 0.2$, and $\alpha = 0.5$ for all experiments if not specified.

4.1 Performance Comparison on Diverse Tasks

LLaVA-1.5-7B First, we compare our method with baselines using LLaVA-1.5-7B, which is a popular benchmark for vision token selection. The model has a fixed number of vision tokens for

Method	GQA	MMB	MME	POPE	SQA	VQA^{V2}	VQA^{Text}	MMMU	SEED	Avg.
Total 576 Tokens										
LLaVA-1.5-7B	61.90	64.70	1862.00	85.90	69.50	78.50	58.20	36.30	58.60	100%
Retain 192 Tokens ↓ 67%										
FastV	52.70	61.20	1612.00	64.80	67.30	67.10	52.50	34.30	57.10	89.6%
SparseVLM	57.60	62.50	1721.00	83.60	69.10	75.60	56.10	33.80	55.80	95.5%
VisionZip	59.30	63.00	1782.60	85.30	68.90	76.80	57.30	36.60	56.40	97.9%
DivPrune	59.97	62.54	1762.23	87.00	68.66	76.87	56.97	35.44	58.71	98.0%
VisionZip 🔥	60.10	63.40	1834.00	84.90	68.20	77.40	57.80	36.20	57.10	98.4%
MMTok	60.07	63.40	1773.86	86.42	68.76	77.11	57.68	36.33	59.21	**98.7%**
Retain 128 Tokens ↓ 78%										
FastV	49.60	56.10	1490.00	59.60	60.20	61.80	50.60	34.90	55.90	84.4%
SparseVLM	56.00	60.00	1696.00	80.50	67.10	73.80	54.90	33.80	53.40	92.9%
VisionZip	57.60	62.00	1761.70	83.20	68.90	75.60	56.80	37.90	54.90	96.8%
DivPrune	59.25	62.03	1718.22	86.72	68.66	75.96	56.06	35.56	56.98	96.9%
VisionZip 🔥	58.90	62.60	1823.00	83.70	68.30	76.60	57.00	37.30	55.80	97.7%
MMTok	59.29	62.29	1779.14	86.25	68.82	76.35	57.03	35.67	58.59	**97.8%**
Retain 64 Tokens ↓ 89%										
FastV	46.10	48.00	1256.00	48.00	51.10	55.00	47.80	34.00	51.90	75.6%
SparseVLM	52.70	56.20	1505.00	75.10	62.20	68.20	51.80	32.70	51.10	86.9%
VisionZip	55.10	60.10	1690.00	77.00	69.00	72.40	55.50	36.20	52.20	93.2%
DivPrune	57.78	59.28	1674.40	85.56	68.07	74.11	54.69	35.56	55.13	94.8%
VisionZip 🔥	57.00	61.50	1756.00	80.90	68.80	74.20	56.00	35.60	53.40	95.0%
MMTok	58.29	61.17	1715.33	85.77	69.16	75.20	56.01	36.11	57.15	**96.6%**

Table 1: **Performance Comparison on LLaVA-1.5-7B.** More details in Appendix Table 16.

Method	LLaVA-1.5-7B (2023)			LLaVA-1.5-13B (2023)			LLaVA-NeXT-7B (2024a)			LLaVA-NeXT-13B (2024a)		
	576 tokens			576 tokens			Upper(Up.) 2880 tokens			Upper(Up.) 2880 tokens		
Compress Ratio	↓ 67%	↓ 78%	↓ 89%	↓ 67%	↓ 78%	↓ 89%	↓ 78%	↓ 89%	↓ 94%	↓ 78%	↓ 89%	↓ 94%
Remain Token	192	128	64	192	128	64	Up. 640	Up. 320	Up. 160	Up. 640	Up. 320	Up. 160
VisionZip	97.9%	96.8%	93.2%	97.9%	97.0%	93.7%	97.5%	94.5%	90.4%	97.7%	94.7%	91.4%
DivPrune	98.0%	96.9%	94.8%	98.2%	96.9%	95.3%	97.1%	95.1%	92.4%	97.1%	94.5%	92.0%
VisionZip 🔥	98.4%	97.7%	95.0%	98.7%	97.4%	94.8%	98.9%	97.6%	95.0%	98.8%	97.8%	94.6%
MMTok	**98.7%**	**97.8%**	**96.6%**	**98.7%**	**97.5%**	**96.4%**	**98.7%**	**97.3%**	**95.1%**	**98.2%**	**96.4%**	**95.1%**

Table 2: **Comparison on LLaVA-1.5 and LLaVA-NeXT.** Details are in Appendix Tables 16 to 19.

arbitrary visual inputs. As shown in Table 1, given the original 576 tokens, MMTok achieves the best performance (preserving on average 98.7/97.8/96.6% original performance of LLaVA-1.5-7B), when retaining only 192/128/64 tokens (reducing by 67/78/89% of tokens compared to 576), respectively. Specifically, our method outperforms DivPrune by 1.8% when using a budget of 64 tokens. Although the gap decreases with more tokens as expected, MMTok still surpasses all baselines without fine-tuning by at least 0.7% with 192 tokens. In addition, compared to the fine-tuning method, the proposed method is 1.6% better than VisionZip🔥 with 64 tokens, which shows the potential of the training-free strategy. Since VisionZip and DivPrune show much better performance than FastV and SparseVLM, we will include only them for comparison in the following experiments.

LLaVA-1.5-13B The average performance over all benchmark datasets and token budgets is reported in Table 2, while detailed results can be found in Appendix Table 17. Although the model is larger, the observation is similar to the above 7B counterpart, where our method consistently outperforms the baselines with a clear margin.

LLaVA-NeXT 7B and 13B In addition to models that have a fixed number of vision tokens, we further evaluate our method on LLaVA-NeXT (Liu et al., 2024a), which dynamically samples up to five images and processes them individually, resulting in up to 2880 vision tokens. To align the comparison with real applications, we keep the dynamic settings as VisionZip (Yang et al., 2025a) and have token selection performed in a fixed ratio. For example, with a maximum budget of 160 tokens, we retain 32 tokens per image in up to five images ($32 \times 5 = 160$). The retained number of tokens becomes 128 if only four images are sampled by the VLMs according to the ratio of $160/2,880$. The same setting is used for all baselines as a fair comparison. As shown in Table 2, our method

retains more than 95% of the original performance using only 5.5% of the tokens with a budget of 160 tokens, indicating substantial redundancy in vision tokens and the effectiveness of the proposed strategy. Detailed results can be found in Appendix Tables 18 and 19.

Method	GQA Acc. ↑	MMB Acc. ↑	MME P+C ↑	POPE F1 ↑	VQA^{Text} Acc. ↑	SQA Acc. ↑	OCRBench Acc. ↑	Avg.† ↑
Dynamic Resolution (MinPix = 256 × 28 × 28, MaxPix = 2048 × 28 × 28), Upper Bound **(100%)**								
Avg. Tokens $\bar{T}$	358.5	276.9	867.6	359.6	976.5	323.0	652.8	
Qwen-2.5-VL-7B	60.48	83.25	2327	86.16	77.72	87.46	83.80	100%
Fixed Resolution (MinPix = MaxPix = 2048 × 28 × 28), Upper Bound **(100%)**								
Qwen-2.5-VL-7B	58.59	83.59	2339	86.09	76.64	86.91	76.60	99.3%
Retain 20% $\bar{T}$	71.7	55.4	173.5	71.9	195.3	64.6	130.6	**↓ 80%**
VisionZip	56.80	80.33	2174	83.38	70.43	84.23	59.50	94.2%
DivPrune	56.70	76.98	2163	80.59	65.86	80.91	48.10	91.5%
MMTok	58.09	79.30	2217	82.38	70.49	81.61	59.60	**94.6%**
Retain 10% $\bar{T}$	35.9	27.7	86.8	36.0	97.7	32.3	65.3	**↓ 90%**
VisionZip	52.47	75.60	2003	78.90	63.78	82.30	36.90	87.5%
DivPrune	53.43	72.85	1957	74.99	59.59	79.57	37.30	84.7%
MMTok	55.09	74.74	2051	78.75	63.90	80.47	43.60	**88.5%**
Retain 5% $\bar{T}$	17.9	13.8	43.4	18.0	48.8	16.2	32.6	**↓ 95%**
VisionZip	46.28	67.53	1677	66.38	54.49	79.57	19.70	75.4%
DivPrune	49.01	65.89	1739	68.45	52.02	77.05	24.90	76.3%
MMTok	50.66	65.89	1796	71.35	55.95	77.19	30.70	**79.0%**
0 Token **↓ 100%**								
Qwen-2.5-VL-7B	31.84	20.10	935	0.00*	38.93	71.10	1.80	33.8%

Table 3: **Comparison on Qwen-2.5-VL-7B.** Avg.† are computed over 5 datasets. *When no visual tokens are provided, Qwen-2.5-VL outputs "No" for all questions, leading to 0% F1. More detailed results are in Appendix Table 20.

Qwen-2.5-VL-7B Finally, we compare different algorithms on a more advanced VLM, that is, Qwen-2.5-VL-7B. Unlike previous work, it adopts dynamic resolution and a token-merging layer. Those strategies help reduce the total number of vision tokens while demonstrating better performance. For example, on POPE the average number of input tokens is only 359.6 in Qwen, significantly less than 2880 tokens in LLaVA-NeXT. Therefore, it is more challenging to apply the token selection algorithm in this stronger model. Following experiments for LLaVA-NeXT, we conduct the evaluation under dynamic resolution for all methods. Due to distinct image pre-processing strategies in Qwen, we include 7 image datasets in this comparison. Since ScienceQA(SQA) is a low-IC dataset that will be discussed in Section 4.2 and all baselines perform poorly on OCRBench, the average performance is computed across the remaining 5 datasets. For MMTok, we reduce τ_t to 0.01 for all datasets while other parameters remained.

First, we compare the dynamic resolution to the fixed number of tokens in Qwen as shown in the first two rows of Table 3. Although the model can use a fixed number of about 2,048 vision tokens for different tasks, the performance is worse than that of the dynamic strategy, which has much fewer tokens. It shows that vision tokens are quite redundant for VLM tasks, and the sophisticated strategies in Qwen already compress the number to hundreds, providing even better performance. Based on the challenging dynamic setting, we further investigate whether token selection is still valuable. From Table 3, we can find that our MMTok can preserve nearly 95% of the original performance while further reducing the number of vision tokens to 20%. This observation demonstrates that even for models with token compression, the remaining tokens can still be redundant. The proposed method MMTok can effectively explore the most informative tokens and further reduce the number of vision tokens from hundreds to tens. Furthermore, our method is better than VisionZip with different budgets, which confirms the efficacy of our proposed multimodal coverage strategy. Finally, we can observe that even without any vision tokens, Qwen's performance on SQA is still close to its version with all tokens. This reminds us to investigate the contribution of vision to vision-language tasks in the next subsection, which can help to better evaluate the performance of token selection methods.

4.2 Comparison on High IC Tasks with Limited Vision Tokens

Although multimodal tasks rely on images for answers, the contribution of vision varies. Table 4 summarizes the performance with/without vision tokens on different datasets. It is interesting to observe that even without any vision tokens, LLaVA-1.5 still preserves 92% of the original

performance on MMMU and 91% on ScienceQA. Those tasks may fail to help adequately assess the efficacy of vision token selection. To mitigate the issue, we introduce **Image Contribution (IC)** to quantify the relative performance gain from all vision tokens, $IC = (\text{Perf}_{\text{All}} - \text{Perf}_0)/\text{Perf}_0$ and summarize IC values in Table 4. According to the table, we can identify 5 and 6 high-IC datasets for LLaVA and LLaVA-NeXT, respectively. Then, we compare different algorithms on those datasets in Table 5. To evaluate the performance with an extremely aggressive compression ratio, we extend the experiments from 64 tokens to 2 tokens. The comparison shows that our method can substantially preserve the informative vision tokens for VL tasks. Moreover, we illustrate the performance ratio compared to the original result in Figure 1. On POPE, our method maintains about 80% original performance with only 2 vision tokens, showing the importance of appropriate vision tokens. More results can be found in Appendix Tables 21 and 22.

Dataset	LLaVA-1.5-7B		LLaVA-NeXT-7B	
	All / Zero	IC	All / Zero	IC
MMB	64.7/19.33	**2.347**	67.9/17.87	**2.801**
POPE	85.9/44.64	**0.924**	86.4/25.84	**2.344**
MME	1862/970.89	**0.918**	1842/867	**1.125**
SEED-I	66.14/37.03	**0.786**	70.2/37.43	**0.875**
GQA	61.9/37.65	**0.644**	64.2/38.23	**0.679**
TextVQA	58.2/41.66	0.397	61.3/37.77	**0.623**
SQA	69.5/63.51	0.094	70.2/64.60	0.087
MMMU	36.3/33.33	0.089	35.1/31.56	0.112

Table 4: Demonstration of Image Contribution (IC).

Model/Method	Different Token Budgets					
	64	32	16	8	4	2
LLaVA-1.5-7B (MMB, POPE, MME, SEED, GQA)						
VisionZip	90.0%	83.5%	69.7%	48.9%	43.8%	43.0%
DivPrune	93.1%	89.6%	81.4%	68.4%	54.3%	50.1%
MMTok (Ours)	**94.7%**	**91.0%**	**86.4%**	**79.8%**	**71.4%**	**62.1%**
LLaVA-NeXT-7B (MMB, POPE, MME, SEED, GQA, TextVQA)						
VisionZip	93.2%	87.5%	76.8%	52.6%	39.4%	38.5%
DivPrune	94.2%	89.7%	85.7%	79.9%	71.0%	57.8%
MMTok (Ours)	**95.7%**	**92.8%**	**89.6%**	**85.2%**	**79.2%**	**71.0%**

Table 5: Comparison on high-IC tasks with different token budgets.

4.3 Ablation Study

We conduct comprehensive ablation studies to demonstrate each component in MMTok. All experiments are performed on LLaVA-1.5-7B with 64 tokens unless otherwise specified.

Multimodal Coverage	GQA Acc. ↑	MMB Acc. ↑	MME P+C ↑	POPE F1 ↑	SQA Acc. ↑	VQA^{Text} Acc. ↑	MMMU Acc. ↑	SEED Acc. ↑	Avg. ↑
Total 576 Tokens **(100%)**									
LLaVA-1.5-7B	61.9	64.7	1862	85.9	69.5	58.2	36.3	58.6	100.0%
Retain 64 Tokens ↓ 88.9%									
T-V (M^{tv})	56.82	59.62	1632.47	83.56	68.72	51.97	35.33	56.36	93.8%
V-V (M^{vv})	58.14	59.88	1662.34	83.43	67.67	53.93	35.33	56.90	94.7%
Softmax T-V ($M^{tv'}$)	56.66	58.85	1674.11	83.69	68.57	52.01	35.33	56.37	93.9%
Softmax V-V ($M^{vv'}$)	57.97	60.31	1684.33	84.31	68.07	55.90	35.89	56.88	95.7%
MMTok ($M^{tv'} + M^{vv'}$)	**58.29**	**61.17**	**1715.33**	**85.77**	**69.16**	**56.01**	**36.11**	**57.15**	**96.7%**

Table 6: **Ablation on multimodal coverage in MMTok**. The best performance with token selection is highlighted in bold and the second-best is underlined.

Model	Upper Token	Total Infer T(s)	POPE Infer T(s)	GPU Util.	Memory (+25.42 GB)	POPE F1	SEED Acc.	TextVQA Acc.	MME P+C	MMB Acc.	GQA Acc.	Avg. (%)
H100 Single GPU Performance, Upper 2880 Tokens												
LLaVA-NeXT-13B	2880	15204	1705	86.7%	4.59	86.22	71.89	64.33	1900.86	69.16	65.38	100.0
VisionZip	Upper 160	7551	866	52.4%	1.92	76.32	61.18	58.33	1738.24	64.78	57.77	89.6
DivPrune	Upper 160	8186	1060	50.9%	1.23	82.16	63.80	54.65	1699.83	64.78	59.34	90.5
MMTok	Upper 160	7768	913	58.0%	1.78	85.11	65.45	55.91	1811.35	65.89	61.94	93.7

Table 7: **Comparison of Inference Efficiency.** All results are reproduced under the same hardware and evaluation settings. The initial memory usage for loading the model is 25.42GB.

Unimodal Coverage vs. Multimodal Coverage The proposed method contains both text-vision coverage (T-V) and vision-vision coverage (V-V). We evaluate each component separately in Table 6. Compared with the original similarity matrix, the softmax variant can obtain a similar or even better performance, which shows that calibration on similarity matrices will not hurt the performance. Then, combining coverage optimization on different modalities shows an improvement of about 1% over unimodal coverage, which demonstrates the complementarity between T-V and V-V coverages for diverse tasks. More ablation experiments can be found in Appendix.

Inference Efficiency Besides effectiveness, we examine efficiency in real scenarios. To mimic real applications, we report the total running time on different datasets in Table 7. First, we profile the computational cost on POPE. Obviously, all token selection methods help reduce the utility percentage of the GPU by about 30%, which shows that pruning is helpful for inference. Then, with a fixed memory cost of 25.42GB for model loading, these methods can also help reduce the usage of running-time memory by more than 58.2% compared to the baseline. This reduction in computation and memory helps significantly improve the inference time on POPE, where both VisionZip and our method can reduce the running time by about 50%. DivPrune runs a little bit slower due to a different strategy for handling multiple crops in its official code. Although our method introduces two subproblems, that is, T-V and V-V to optimize, the running time is almost the same as the fast unimodal method, i.e., VisionZip, which confirms the efficiency of MMTok. The running time accumulated over 6 tasks demonstrates a similar phenomenon, where the performance of MMTok is better than VisionZip by 4.1%. This further demonstrates the efficacy and efficiency of our proposal.

Visualization While MMTok will leverage text information for vision token selection, the vision-vision coverage in our framework can help reuse the selected vision tokens for multi-turn conversation as shown in Figure 3. We can observe that MMTok selects tokens with text from Q1 but vision-vision coverage helps the following questions to be answered correctly with the selected vision tokens.

In addition, we also demonstrate how the answer changes with the number of selected tokens in Figure 4. Given a simple question as in the first example, only 8 vision tokens can obtain the right answer. However, for the challenging question as in the last example, the answer changes even with 16 tokens. The phenomenon implies that the appropriate number of vision tokens also depends on the hardness of the questions. Hardness-aware vision token selection is an interesting future direction.

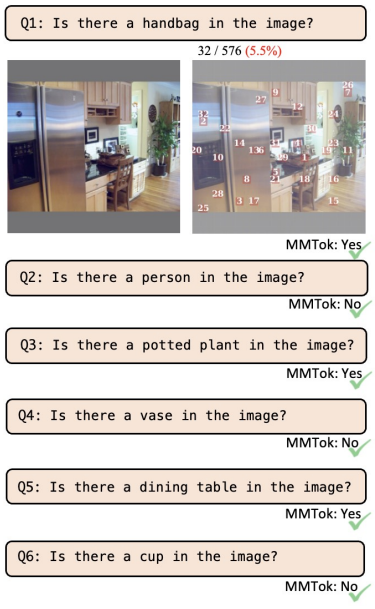

Figure 3: Multi-turn conversation by applying MMTok only with text from Q1.

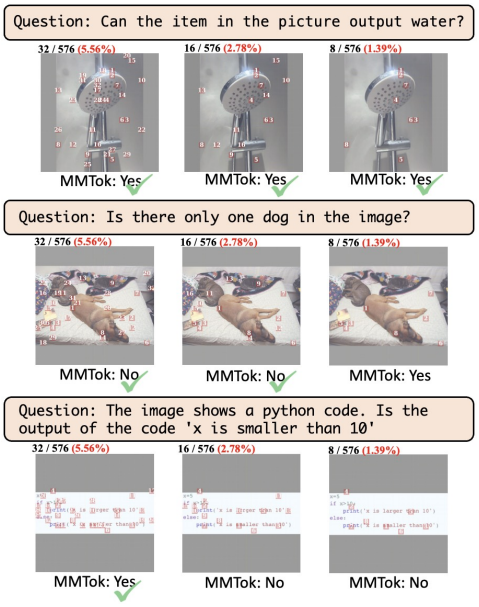

Figure 4: Answer changes with different number of tokens. Hard questions need more vision tokens.

5 Conclusion

In this work, we propose a multimodal coverage framework, MMTok, to guide vision token selection to accelerate the inference of VLMs in a training-free manner. Extensive experiments on benchmark datasets and representative VLMs demonstrate that our method outperforms the unimodal baselines without compromising efficiency. While text input may carry limited semantic information as a target for vision tokens to cover, a lightweight agent VLM can be leveraged to provide additional meaningful text tokens to guide the selection of the vision tokens, which will be an interesting future direction.

6 ETHICS STATEMENT

To the best of our knowledge, this work has no potential ethical issues to disclose.

7 REPRODUCIBILITY STATEMENT

To ensure the reproducibility of this work, all implementation details have been clearly described, and we will also release the code upon acceptance.

REFERENCES

Saeed Ranjbar Alvar, Gursimran Singh, Mohammad Akbari, and Yong Zhang. Divprune: Diversity-based visual token pruning for large multimodal models. In Proceedings of the Computer Vision and Pattern Recognition Conference, pp. 9392–9401, 2025.

Shuai Bai, Keqin Chen, Xuejing Liu, Jialin Wang, Wenbin Ge, Sibo Song, Kai Dang, Peng Wang, Shijie Wang, Jun Tang, et al. Qwen2. 5-vl technical report. arXiv preprint arXiv:2502.13923, 2025.

Daniel Bolya, Cheng-Yang Fu, Xiaoliang Dai, Peizhao Zhang, Christoph Feichtenhofer, and Judy Hoffman. Token merging: Your vit but faster. arXiv preprint arXiv:2210.09461, 2022.

Liang Chen, Haozhe Zhao, Tianyu Liu, Shuai Bai, Junyang Lin, Chang Zhou, and Baobao Chang. An image is worth 1/2 tokens after layer 2: Plug-and-play inference acceleration for large vision-language models. In European Conference on Computer Vision, pp. 19–35. Springer, 2024a.

Lin Chen, Jinsong Li, Xiaoyi Dong, Pan Zhang, Yuhang Zang, Zehui Chen, Haodong Duan, Jiaqi Wang, Yu Qiao, Dahua Lin, et al. Are we on the right way for evaluating large vision-language models? arXiv preprint arXiv:2403.20330, 2024b.

Wenliang Dai, Junnan Li, Dongxu Li, Anthony Tiong, Junqi Zhao, Weisheng Wang, Boyang Li, Pascale N Fung, and Steven Hoi. Instructblip: Towards general-purpose vision-language models with instruction tuning. Advances in neural information processing systems, 36:49250–49267, 2023.

Chaoyou Fu, Peixian Chen, Yunhang Shen, Yulei Qin, Mengdan Zhang, Xu Lin, Jinrui Yang, Xiawu Zheng, Ke Li, Xing Sun, et al. MME: A comprehensive evaluation benchmark for multimodal large language models. arXiv:2306.13394, 2023.

Yash Goyal, Tejas Khot, Douglas Summers-Stay, Dhruv Batra, and Devi Parikh. Making the v in vqa matter: Elevating the role of image understanding in visual question answering. In Proceedings of the IEEE conference on computer vision and pattern recognition, pp. 6904–6913, 2017.

Dong Guo, Faming Wu, Feida Zhu, Fuxing Leng, Guang Shi, Haobin Chen, Haoqi Fan, Jian Wang, Jianyu Jiang, Jiawei Wang, et al. Seed1. 5-vl technical report. arXiv preprint arXiv:2505.07062, 2025.

Kaiming He, Xinlei Chen, Saining Xie, Yanghao Li, Piotr Dollár, and Ross Girshick. Masked autoencoders are scalable vision learners. In Proceedings of the IEEE/CVF Conference on Computer Vision and Pattern Recognition, pp. 16000–16009, 2022.

Drew A Hudson and Christopher D Manning. GQA: A new dataset for real-world visual reasoning and compositional question answering. Conference on Computer Vision and Pattern Recognition (CVPR), 2019.

Sarthak Jain and Byron C Wallace. Attention is not explanation. arXiv preprint arXiv:1902.10186, 2019.

Samir Khuller, Anna Moss, and Joseph Naor. The budgeted maximum coverage problem. Inf. Process. Lett., 70(1):39–45, 1999.

Jure Leskovec, Andreas Krause, Carlos Guestrin, Christos Faloutsos, Jeanne M. VanBriesen, and Natalie S. Glance. Cost-effective outbreak detection in networks. In Proceedings of the 13th ACM SIGKDD International Conference on Knowledge Discovery and Data Mining, San Jose, California, USA, August 12-15, 2007, pp. 420–429. ACM, 2007.

Bo Li, Peiyuan Zhang, Kaichen Zhang, Fanyi Pu, Xinrun Du, Yuhao Dong, Haotian Liu, Yuanhan Zhang, Ge Zhang, Chunyuan Li, and Ziwei Liu. Lmms-eval: Accelerating the development of large multimodal models. https://github.com/EvolvingLMMs-Lab/lmms-eval, March 2024a. Version v0.1.0, Zenodo.

Bohao Li, Rui Wang, Guangzhi Wang, Yuying Ge, Yixiao Ge, and Ying Shan. Seed-bench: Benchmarking multimodal llms with generative comprehension. arXiv preprint arXiv:2307.16125, 2023a.

Yanwei Li, Yuechen Zhang, Chengyao Wang, Zhisheng Zhong, Yixin Chen, Ruihang Chu, Shaoteng Liu, and Jiaya Jia. Mini-gemini: Mining the potential of multi-modality vision language models. arXiv:2403.18814, 2024b.

Yifan Li, Yifan Du, Kun Zhou, Jinpeng Wang, Wayne Xin Zhao, and Ji-Rong Wen. Evaluating object hallucination in large vision-language models. arXiv:2305.10355, 2023b.

Haotian Liu, Chunyuan Li, Yuheng Li, and Yong Jae Lee. Improved baselines with visual instruction tuning. arXiv:2310.03744, 2023.

Haotian Liu, Chunyuan Li, Yuheng Li, Bo Li, Yuanhan Zhang, Sheng Shen, and Yong Jae Lee. Llava-next: Improved reasoning, ocr, and world knowledge, January 2024a. URL https://llava-vl.github.io/blog/2024-01-30-llava-next/.

Haotian Liu, Chunyuan Li, Qingyang Wu, and Yong Jae Lee. Visual instruction tuning. Advances in Neural Information Processing Systems, 2024b.

Yuan Liu, Haodong Duan, Yuanhan Zhang, Bo Li, Songyang Zhang, Wangbo Zhao, Yike Yuan, Jiaqi Wang, Conghui He, Ziwei Liu, et al. Mmbench: Is your multi-modal model an all-around player? In European conference on computer vision, pp. 216–233. Springer, 2024c.

Pan Lu, Swaroop Mishra, Tanglin Xia, Liang Qiu, Kai-Wei Chang, Song-Chun Zhu, Oyvind Tafjord, Peter Clark, and Ashwin Kalyan. Learn to explain: Multimodal reasoning via thought chains for science question answering. Advances in Neural Information Processing Systems, 35:2507–2521, 2022.

George L Nemhauser, Laurence A Wolsey, and Marshall L Fisher. An analysis of approximations for maximizing submodular set functions—i. Mathematical programming, 14(1):265–294, 1978.

Qi Qian, Yuanhong Xu, and Juhua Hu. Intra-modal proxy learning for zero-shot visual categorization with CLIP. In Advances in Neural Information Processing Systems 36: Annual Conference on Neural Information Processing Systems 2023, NeurIPS 2023, New Orleans, LA, USA, December 10 - 16, 2023, 2023.

Alec Radford, Jong Wook Kim, Chris Hallacy, Aditya Ramesh, Gabriel Goh, Sandhini Agarwal, Girish Sastry, Amanda Askell, Pamela Mishkin, Jack Clark, et al. Learning transferable visual models from natural language supervision. In International Conference on Machine Learning, pp. 8748–8763. PMLR, 2021a.

Alec Radford, Jong Wook Kim, Chris Hallacy, Aditya Ramesh, Gabriel Goh, Sandhini Agarwal, Girish Sastry, Amanda Askell, Pamela Mishkin, Jack Clark, et al. Learning transferable visual models from natural language supervision. In International conference on machine learning, pp. 8748–8763. PMLR, 2021b.

Yuzhang Shang, Mu Cai, Bingxin Xu, Yong Jae Lee, and Yan Yan. Llava-prumerge: Adaptive token reduction for efficient large multimodal models. arXiv preprint arXiv:2403.15388, 2024.

Amanpreet Singh, Vivek Natarajan, Meet Shah, Yu Jiang, Xinlei Chen, Dhruv Batra, Devi Parikh, and Marcus Rohrbach. Towards vqa models that can read. In Proceedings of the IEEE/CVF conference on computer vision and pattern recognition, pp. 8317–8326, 2019.

Chameleon Team. Chameleon: Mixed-modal early-fusion foundation models. arXiv preprint arXiv:2405.09818, 2024.

Gemini Team, Rohan Anil, Sebastian Borgeaud, Yonghui Wu, Jean-Baptiste Alayrac, Jiahui Yu, Radu Soricut, Johan Schalkwyk, Andrew M Dai, Anja Hauth, et al. Gemini: a family of highly capable multimodal models. arXiv:2312.11805, 2023.

Ashish Vaswani, Noam Shazeer, Niki Parmar, Jakob Uszkoreit, Llion Jones, Aidan N. Gomez, Lukasz Kaiser, and Illia Polosukhin. Attention is all you need. In Advances in Neural Information Processing Systems 30: Annual Conference on Neural Information Processing Systems 2017, December 4-9, 2017, Long Beach, CA, USA, pp. 5998–6008, 2017.

Sarah Wiegreffe and Yuval Pinter. Attention is not not explanation. arXiv preprint arXiv:1908.04626, 2019.

Senqiao Yang, Yukang Chen, Zhuotao Tian, Chengyao Wang, Jingyao Li, Bei Yu, and Jiaya Jia. Visionzip: Longer is better but not necessary in vision language models. In Proceedings of the Computer Vision and Pattern Recognition Conference, pp. 19792–19802, 2025a.

Senqiao Yang, Junyi Li, Xin Lai, Bei Yu, Hengshuang Zhao, and Jiaya Jia. Visionthink: Smart and efficient vision language model via reinforcement learning. arXiv preprint arXiv:2507.13348, 2025b.

Xiang Yue, Yuansheng Ni, Kai Zhang, Tianyu Zheng, Ruoqi Liu, Ge Zhang, Samuel Stevens, Dongfu Jiang, Weiming Ren, Yuxuan Sun, et al. Mmmu: A massive multi-discipline multimodal understanding and reasoning benchmark for expert agi. In Proceedings of the IEEE/CVF Conference on Computer Vision and Pattern Recognition, pp. 9556–9567, 2024.

Yuan Zhang, Chun-Kai Fan, Junpeng Ma, Wenzhao Zheng, Tao Huang, Kuan Cheng, Denis Gudovskiy, Tomoyuki Okuno, Yohei Nakata, Kurt Keutzer, et al. Sparsevlm: Visual token sparsification for efficient vision-language model inference. arXiv preprint arXiv:2410.04417, 2024.

A LLM USAGE STATEMENT

We did not use LLM at all during the idea and writing stage of this work.

B EXPERIMENTS

B.1 ADAPTIVE TEMPERATURE τ_v^a

To further improve the calibration between $M^{tv'}$ and $M^{vv'}$, an adaptive visual temperature can be applied for each example. Concretely, when fixing τ_t, the maximal similarity between the target text tokens and the whole set of vision tokens can be obtained as $f(\mathcal{N}; M^{tv'})$, letting $\mathcal{S} = \mathcal{N}$. The desired temperature τ_v should lead to a similar magnitude for the vision-vision similarity. The optimization problem can be cast as

$$\min_{\tau_v^a} |f(\mathcal{N}; M^{tv'}) - f(\mathcal{N}; M^{vv'})|$$

For the default f, it is monotone to τ_v^a, which can be solved efficiently by bisection search. However, the diagonal elements in $M^{vv'}$ can mislead the optimization due to their fixed value of 1. To mitigate the issue, the k-th largest value is applied to search for the temperature as

$$\min_{\tau_v^a} |f(\mathcal{N}; M^{tv'}) - f_k(\mathcal{N}; M^{vv'})|; \quad f_k(\mathcal{N}; M^{vv'}) = \frac{1}{n}\sum_{i=1}^{n} \max_k M_{i,:}^{vv'}$$

Moreover, f_k is not guaranteed to be a monotone function to τ_v^a , and we can search the value in $(\tau_t, \tau_v]$ as suggested in (Qian et al., 2023), where it shows that the temperature between vision-vision should be higher than that between text-vision due to the modality gap.

We perform the evaluation on high IC tasks in Table 8. As discussed above, the second largest value is adopted for searching the temperature in the set of $\{0.05, 0.1, 0.15, 0.2\}$. While the variant with adaptive temperature, i.e., $\text{MMTok}_{\text{Adapt}}$, shows a slightly better performance with a budget of 16 tokens, the results over different tasks are almost the same, demonstrating that our method is insensitive to hyperparameters.

Method	GQA Acc. ↑	MMB Acc. ↑	POPE F1 ↑	MME P+C ↑	SEED Acc. ↑	Avg. ↑
Upper Bound: LLaVA-1.5-7B (576 Tokens)						
LLaVA-1.5 7B	61.9	64.7	85.9	1862	58.6	100%
Retain 16 Tokens ↓ 97.2%						
MMTok	53.31	54.30	79.79	1550.65	56.67	88.6%
$\text{MMTok}_{\text{Adapt}}$	53.31	54.30	79.83	1565.10	56.66	88.7%

Table 8: **Fixed vs. Adaptive Temperature.** Evaluation on LLaVA-1.5 7B with adaptive temperature $\tau_v^a \in \{0.05, 0.1, 0.15, 0.2\}$.

B.2 POOLING STRATEGY FOR TEXT

Given an LLM, each word can be tokenized into multiple tokens. To recover the semantic information of words, we may aggregate tokens from the same word. In this experiment, we explore different pooling strategies when computing T-V similarity. Concretely, we consider the pooling process either before or after computing the similarity matrix, where `Max`-pooling selects the token with the maximum feature value or similarity, `Mean`-pooling averages similarity over all tokens, and `First`-pooling simply retains the first token of a word. As shown in Table 9, there is no pooling strategy that consistently yields the best performance across all eight datasets. Therefore, our method does not apply word pooling for simplicity.

B.3 MMTOK FOR REASONING TASK

To demonstrate the efficacy of MMTok on reasoning task, we conduct the experiments on the MMStar dataset Chen et al. (2024b). In Table 10, we can observe that vision token selection can also help

Pooling Method	Position	GQA Acc. ↑	MMB Acc. ↑	MME P+C ↑	POPE F1 ↑	SQA Acc. ↑	VQA^{Text} Acc. ↑	MMMU Acc. ↑	SEED Acc. ↑	Avg. ↑
MMTok on LLaVA-1.5-7B with 64 Tokens (Baseline)										
None	-	58.29	61.17	**1715**	**85.77**	**69.16**	**56.01**	36.11	57.15	**100.0%**
Pre-Pooling (Before Similarity Calculation)										
Mean	Pre	58.01	61.00	1703	85.75	69.11	55.73	36.00	57.13	99.7%
Max	Pre	58.26	61.17	1704	85.64	68.82	55.82	35.89	56.94	99.7%
First	Pre	**58.39**	**61.34**	1709	85.67	68.77	55.76	36.11	56.90	99.8%
Post-Pooling (After Similarity Calculation)										
Mean	Post	58.20	61.00	1690	85.67	68.77	55.77	**36.22**	**57.16**	99.7%
Max	Post	58.36	61.00	1711	85.61	68.77	55.68	**36.22**	57.04	99.8%
First	Post	**58.39**	**61.34**	1709	85.67	68.77	55.76	36.11	56.90	99.8%

Table 9: **Word token pooling strategies for token selection on LLaVA-1.5-7B.** Pre-pooling aggregates subword tokens before similarity computation, while post-pooling applies pooling afterward. We evaluate three methods: `Mean` (average pooling), `Max` (maximum pooling), and `First` (first subword). The baseline applies no pooling. The best is in bold and the second-best is underlined.

reasoning tasks. It should be noted that the major issue on these challenging tasks is that the original performance without selection is already quite low. Therefore, it is hard to show the significant difference when the upper-bound is limited. Nevertheless, our method is still better than baselines with a clear margin and by selecting 32 out of 576 tokens, MMTok is able to recover the performance of the baseline.

Method	MMStar Metrics						
	Coarse	Fine-Grained	Instance	Logical	Math	Sci&Tech	Average
Baseline							
LLaVA-1.5-7B	63.63	25.63	38.89	28.92	26.60	18.48	33.69
64 Tokens							
VisionZip	55.27	22.92	39.32	27.95	24.76	24.62	32.47
DivPrune	56.35	19.50	36.72	27.73	26.70	18.94	30.99
Ours	59.08	22.66	39.51	29.66	28.39	20.66	33.33
32 Tokens							
VisionZip	48.58	19.04	39.73	29.69	22.91	21.95	30.32
DivPrune	54.82	21.07	37.03	27.82	24.18	19.32	30.71
Ours	59.56	25.71	40.49	29.94	27.92	17.37	33.50
16 Tokens							
VisionZip	43.76	21.34	32.58	25.97	23.18	19.96	27.80
DivPrune	49.99	21.45	38.37	28.45	21.54	18.58	29.73
Ours	56.32	21.58	39.48	30.22	23.98	15.16	31.12
8 Tokens							
VisionZip	27.93	21.26	25.71	21.84	20.18	17.83	22.46
DivPrune	47.25	21.05	33.89	25.75	20.32	16.76	27.50
Ours	54.11	21.26	35.09	29.56	20.34	15.04	29.23
0 Tokens							
Baseline	31.85	19.10	23.77	23.61	14.28	16.11	21.45

Table 10: Comparison on MMStar with LLaVA-1.5-7B.

B.4 MMTok vs. Resizing

Resizing image resolution is an effective way to reduce the total number of tokens as shown in Yang et al. (2025b). We compare the resize strategy with token budgets in Table 11. It shows that selecting vision tokens from the original large image can be more effective than resizing under the

same token budget. This is because resizing would ignore the redundancy between vision tokens. More importantly, we observe that incorporating with resizing, MMTok can work better than the counterpart with the same token budget on full images. For example, with about 10% original tokens, MMTok with resizing can achieve 2170 on MME while that on original image is only 2051. Exploring resizing with token selection sufficiently can be our future work.

Model	Image Resize Ratio	Token Avg.	MME P+C ↑
Qwen2.5-VL-7B	1	867.6	2327
MMTok	1	86.8	2051
MMTok	1	173.5	2217
Resize image to fixed ratio of original height and width, respectively			
Qwen2.5-VL-7B	1/2	459.1	2274
Qwen2.5-VL-7B	1/4	349.6	2238
Qwen2.5-VL-7B	1/8	276.0	1793
Retain *55%* Tokens on $1/4$ Resized Image			
MMTok	1/4	192.3	2254
Retain *40%* Tokens on $1/4$ Resized Image			
MMTok	1/4	139.8	2215
Retain *25%* Tokens on $1/4$ Resized Image			
MMTok	1/4	87.4	2170

Table 11: Comparison with resize strategy on MME with Qwen2.5-VL-7B. The original image is denoted as resize ratio of 1. Qwen has a default minimal number of vision tokens as 256 to obtain meaningful results.

B.5 Inference Efficiency for Qwen2.5-VL-7B

Besides the evaluation in Table 7, we also evaluate the inference efficiency of Qwen2.5-VL-7B in Table 12 using the MME task. We find that vision token selection can also accelerate the inference of state-of-the-art VLMs.

Model	Token Avg.	Inference Time(s)	GPU. util.	Memory (+15.87GB)
1 × A6000 GPU Performance on MME				
Qwen2.5-VL-7B	867.6	675	77.0%	3.05
VisionZip	86.8	508	66.3%	0.41
DivPrune	86.8	423	55.1%	0.71
MMTok	86.8	419	60.0%	0.71

Table 12: **Comparison of Inference Efficiency on Qwen2.5-VL-7B**. The initial memory usage for loading the model is 15.87GB.

B.6 Efficiency effect of the number of input or selected vision tokens

In MMTok, the similarity matrix can be constructed efficiently using the pytorch built-in libraries. Then, for token selection, MMTok proposes a greedy algorithm only with max operations and can run in $O(kn)$ to pick k vision tokens, where n is the total number of vision tokens. Therefore, our method can scale well with vision tokens and with the number of selected vision tokens. In Table 13, we show the running time of MMTok with the varying number of input and selected vision tokens. We find that with the same number of input tokens, the running time is almost linear in the number of selected tokens, which confirms our analysis. Moreover, even with 2880 input tokens, the running time of MMTok is less than 7ms, which is negligible for real applications. It should also be noted that even for 2880 input tokens, the computation only costs about 13.93 GFLOPs.

#Input	#Select	Time(ms)	#Input	#Select	Time(ms)	#Input	#Select	Time(ms)
2880	160	6.417	1728	96	3.862	576	32	1.267
2880	80	3.733	1728	48	2.247	576	16	0.774

Table 13: Running time (ms) of MMTok with different numbers of input and selected vision tokens on LLaVA-NeXT-7B. The reported result is averaged over 100 runs on a A6000 GPU.

B.7 Token Selection in Decoder

Following the common practice, token selection has been conducted mainly after the vision encoder. In fact, token selection can also happen in the decoder. We conduct a preliminary experiment on the decoder in Table 14. We try to further select the vision tokens from 160 to 80 for an intermediate layer (i.e., L-24) of the decoder in LLaVA-Next on MME. We can find that it can keep the similar performance and further improve the token efficiency.

Model	Upper Tokens	MME P+G ↑
LLaVA-Next-13B	2880	1901
MMTok	160	1811
MMTok	160⇒80 (L24)	1846
MMTok	80	1717

Table 14: Comparison with vision token selection during decoding. We have an additional vision token selection in the 24th layer of decoder.

C Improved MMTok

Since LLaVA-1.5 does not fine-tune the vision tower and also does not mask padding patches, we explicitly exclude padding patches from the candidate token set and fix an overflow bug that wasted one token. As shown in Table 15, these changes substantially improve accuracy while using fewer tokens.

D Selected Tokens Visualization

To provide an intuitive understanding of our token selection process, we visualize the selected tokens and their nearest words in Figure 5 and compare them with the diversity-based method, DivPrune. From the columns (b) and (c), we can observe that MMTok selects top patches according to the word to patch similarity, which aligns well with the question semantically. In contrast, as shown in columns (d) and (e), DivPrune selected top patches without any close semantic relation to the question. This further demonstrates that MMTok can help significantly reduce the number of tokens without losing the semantic relation to the questions, so as to provide better performance.

E Complete Empirical Results

This section shows per-dataset results for all models and token budgets, including LLaVA-1.5 (7B/13B) (Tables 16 and 17), LLaVA-NeXT (7B/13B) (Tables 18 and 19), and Qwen-2.5-VL (7B Table 20). We report both raw scores and percentage retention relative to the full-token setting. We also report results with an extremely low number of tokens on LLaVA-1.5-7B and LLaVA-NeXT-7B (Tables 21 and 22).

Method	GQA Acc. ↑	MMB Acc. ↑	MME P+C ↑	POPE F1 ↑	SEED-I Acc. ↑	Avg ↑
Vanilla Baseline (576 tokens)						
LLaVA-1.5-7B	61.9	64.7	1862	85.9	66.14	100.0%
32 Tokens						
MMTok	55.95	58.59	1625	82.95	59.81	91.0%
MMTok++	56.61	58.76	1636	83.44	59.85	91.6%
16 Tokens						
MMTok	53.31	54.30	1551	79.79	56.67	86.4%
MMTok++	54.05	54.98	1581	80.79	57.13	87.5%
8 Tokens						
MMTok	49.06	49.06	1355	78.46	52.74	79.8%
MMTok++	50.80	49.31	1395	79.75	53.59	81.4%
4 Tokens						
MMTok	43.93	36.94	1290	74.84	48.10	71.4%
MMTok++	45.08	40.21	1294	76.36	49.34	73.6%
2 Tokens						
MMTok	40.58	25.69	1122	68.95	42.89	62.1%
MMTok++	42.18	31.36	1237	72.97	45.27	67.3%
0 Tokens						
Baseline	37.65	19.33	971	44.64	37.03	50.2%

Table 15: Evaluate MMTok++ on LLaVA-1.5-7B with Extremely Less Token Budgets.

Question: Is there a traffic light in the image? Answer the question using a single word or phrase.

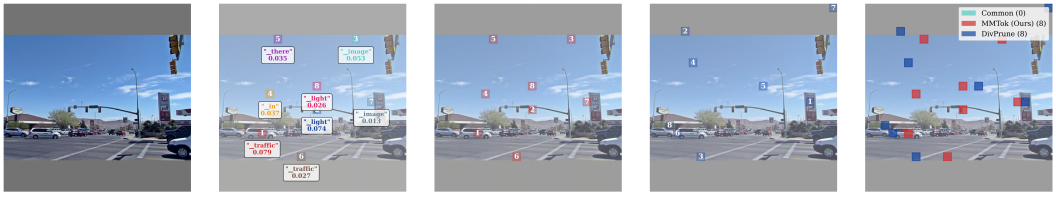

(a) Original Image (b) Words-To-Patches Similarity (c) MMTok (d) DivPrune (e) MMTok vs DivPrune

Question: Is there a chair in the image? Answer the question using a single word or phrase.

(a) Original Image (b) Words-To-Patches Similarity (c) MMTok (d) DivPrune (e) MMTok vs DivPrune

Question: Is there a clock in the image? Answer the question using a single word or phrase.

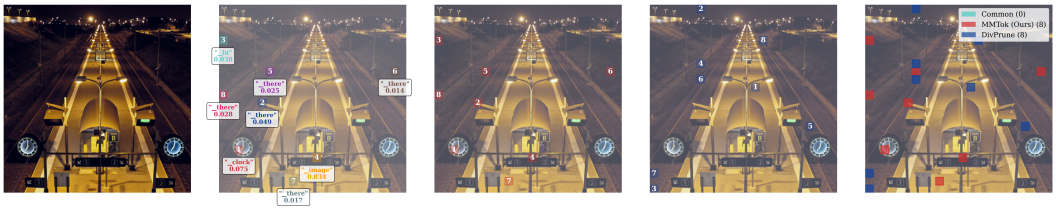

(a) Original Image (b) Words-To-Patches Similarity (c) MMTok (d) DivPrune (e) MMTok vs DivPrune

Question: Is there a person in the image? Answer the question using a single word or phrase.

(a) Original Image (b) Words-To-Patches Similarity (c) MMTok (d) DivPrune (e) MMTok vs DivPrune

Question: Is there a chair in the image? Answer the question using a single word or phrase.

(a) Original Image (b) Words-To-Patches Similarity (c) MMTok (d) DivPrune (e) MMTok vs DivPrune

Question: Is there an orange in the image? Answer the question using a single word or phrase.

(a) Original Image (b) Words-To-Patches Similarity (c) MMTok (d) DivPrune (e) MMTok vs DivPrune

Figure 5: **Visualization of Selected Tokens.** Compared with the diversity-based method, DivPrune, our method selected token coverage the necessary token associate to language context.

Method	GQA Acc. ↑	MMB Acc. ↑	MME P+C ↑	POPE F1 ↑	SQA Acc. ↑	VQA^{V2} Acc. ↑	VQA^{Text} Acc. ↑	MMMU Acc. ↑	SEED Acc. ↑	Avg. ↑
Upper Bound, 576 Tokens **(100%)**										
LLaVA-1.5 Vanilla 7B	61.9 100%	64.7 100%	1862 100%	85.9 100%	69.5 100%	78.5 100%	58.2 100%	36.3 100%	58.6 100%	100%
Retain 192 Tokens ↓ 66.7%										
FastV (2024a)	52.7 85.1%	61.2 94.6%	1612 86.6%	64.8 75.4%	67.3 96.8%	67.1 85.5%	52.5 90.2%	34.3 94.5%	57.1 97.4%	89.6%
SparseVLM (2024)	57.6 93.1%	62.5 96.6%	1721 92.4%	83.6 97.3%	69.1 99.4%	75.6 96.3%	56.1 96.4%	33.8 93.1%	55.8 95.2%	95.5%
VisionZip (2025a)	59.3 95.8%	63.0 97.4%	1782.6 95.7%	85.3 99.3%	68.9 99.1%	76.8 97.8%	57.3 98.5%	36.6 100.8%	56.4 96.2%	97.9%
DivPrune (2025)	59.97 96.9%	62.54 96.7%	1762.23 94.6%	87.00 101.3%	68.66 98.8%	76.87 97.9%	56.97 97.9%	35.44 97.6%	58.71 100.2%	98.0%
VisionZip 🔥 (2025a)	60.1 97.1%	63.4 98.0%	1834 98.5%	84.9 98.8%	68.2 98.1%	77.4 98.6%	57.8 99.3%	36.2 99.7%	57.1 97.4%	98.4%
MMTok (Ours)	60.07 97.0%	63.40 98.0%	1773.86 95.3%	86.42 100.6%	68.76 98.9%	77.11 98.2%	57.68 99.1%	36.33 100.1%	59.21 101.0%	**98.7%**
Retain 128 Tokens ↓ 77.8%										
FastV (2024a)	49.6 80.1%	56.1 86.7%	1490 80.0%	59.6 69.4%	60.2 86.6%	61.8 78.7%	50.6 86.9%	34.9 96.1%	55.9 95.4%	84.4%
SparseVLM (2024)	56.0 90.5%	60.0 92.7%	1696 91.1%	80.5 93.7%	67.1 96.5%	73.8 94.0%	54.9 94.3%	33.8 93.1%	53.4 91.1%	92.9%
VisionZip (2025a)	57.6 93.1%	62.0 95.8%	1761.7 94.6%	83.2 96.9%	68.9 99.1%	75.6 96.3%	56.8 97.6%	37.9 104.4%	54.9 93.7%	96.8%
DivPrune (2025)	59.25 95.7%	62.03 95.9%	1718.22 92.3%	86.72 101.0%	68.66 98.8%	75.96 96.8%	56.06 96.3%	35.56 98.0%	56.98 97.3%	96.9%
VisionZip 🔥 (2025a)	58.9 95.2%	62.6 96.8%	1823 97.9%	83.7 97.4%	68.3 98.3%	76.6 97.6%	57.0 97.9%	37.3 102.8%	55.8 95.2%	97.7%
MMTok (Ours)	59.29 95.8%	62.29 96.3%	1779.14 95.5%	86.25 100.4%	68.82 99.0%	76.35 97.3%	57.03 98.0%	35.67 98.3%	58.59 100.0%	**97.8%**
Retain 64 Tokens ↓ 88.9%										
FastV (2024a)	46.1 74.5%	48.0 74.2%	1256 67.5%	48.0 55.9%	51.1 73.5%	55.0 70.1%	47.8 82.1%	34.0 93.7%	51.9 88.6%	75.6%
SparseVLM (2024)	52.7 85.1%	56.2 86.9%	1505 80.8%	75.1 87.4%	62.2 89.4%	68.2 86.9%	51.8 89.0%	32.7 90.1%	51.1 87.2%	86.9%
VisionZip (2025a)	55.1 89.0%	60.1 92.9%	1690 90.8%	77.0 89.6%	69.0 99.3%	72.4 92.2%	55.5 95.4%	36.2 99.7%	52.2 89.1%	93.2%
DivPrune (2025)	57.78 93.3%	59.28 91.6%	1674.4 89.9%	85.56 99.6%	68.07 97.9%	74.11 94.4%	54.69 94.0%	35.56 98.0%	55.13 94.1%	94.8%
VisionZip 🔥 (2025a)	57.0 92.1%	61.5 95.1%	1756 94.3%	80.9 94.2%	68.8 99.0%	74.2 94.5%	56.0 96.2%	35.6 98.1%	53.4 91.1%	95.0%
MMTok (Ours)	58.29 94.2%	61.17 94.5%	1715.33 92.1%	85.77 99.9%	69.16 99.5%	75.20 95.8%	56.01 96.3%	36.11 99.5%	57.15 97.5%	**96.6%**

Table 16: **Performance Comparison on LLaVA-1.5-7B.** The vanilla number of visual tokens is 576. The first line of each method shows the raw benchmark accuracy, and the second line is the proportion relative to the upper limit. The last column is the average value.

Method	GQA Acc. ↑	MMB Acc. ↑	MME P+C ↑	POPE F1 ↑	SQA Acc. ↑	VQA^{V2} Acc. ↑	VQA^{Text} Acc. ↑	MMMU Acc. ↑	SEED-I Acc. ↑	SEED* Acc. ↑	Avg. ↑
Upper Bound, 576 Tokens **(100%)**											
LLaVA-1.5 Vanilla 13B	63.2 100%	67.7 100%	1818 100%	85.9 100%	72.8 100%	80.0 100%	61.3 100%	36.4 100%	66.9 100%	61.6 100%	100%
Retain 192 Tokens ↓ 66.7%											
VisionZip (2025a)	59.1 93.5%	66.9 98.8%	1754 96.5%	85.1 99.1%	73.5 101.0%	78.1 97.6%	59.5 97.1%	36.4 100%	65.2 97.5%	61.20† 99.4%	97.9%
DivPrune (2025)	59.42 94.0%	66.58 98.3%	1781.50 98.0%	86.76 101.0%	73.03 100.3%	77.98 97.5%	58.46 95.4%	36.56 100.4%	65.72 98.2%	60.83 98.8%	98.2%
VisionZip 🔥 (2025a)	61.6 97.5%	67.1 99.1%	1790 98.5%	84.5 98.4%	72.7 99.9%	78.6 98.3%	59.9 97.7%	36.4 100%	66.1 98.8%	– –	98.7%
MMTok (Ours)	59.67 94.4%	67.70 100.0%	1784.16 98.1%	86.15 100.3%	73.62 101.1%	78.30 97.9%	59.64 97.3%	36.78 101.0%	65.49 97.9%	61.17 99.3%	**98.7%**
Retain 128 Tokens ↓ 77.8%											
VisionZip (2025a)	57.9 91.6%	66.7 98.5%	1743 95.9%	85.2↓ 99.2%	74.0 101.6%	76.8 96.0%	58.7 95.8%	36.1 99.2%	63.8 95.4%	59.74† 97.0%	97.0%
DivPrune (2025)	58.89 93.2%	66.07 97.6%	1748.56 96.2%	86.53 100.7%	72.48 99.6%	77.10 96.4%	58.17 94.9%	35.56 97.7%	64.22 96.0%	59.49 96.6%	96.9%
VisionZip 🔥 (2025a)	60.1 95.1%	67.6 99.9%	1736 95.5%	83.8 97.6%	73.0 100.3%	77.6 97.0%	59.2 96.6%	35.4 97.3%	64.9 97.0%	– –	97.4%
MMTok (Ours)	58.98 93.3%	67.18 99.2%	1756.20 96.6%	86.22 100.4%	73.38 100.8%	77.57 97.0%	59.22 96.6%	35.44 97.4%	64.26 96.1%	60.11 97.6%	**97.5%**
Retain 64 Tokens ↓ 88.9%											
VisionZip (2025a)	56.2 88.9%	64.9 95.9%	1676 92.2%	76.0 88.5%	74.4 102.2%	73.7 92.1%	57.4 93.6%	36.4 100%	60.4 90.3%	57.13† 92.7%	93.7%
DivPrune (2025)	57.66 91.2%	64.60 95.4%	1777.93 97.8%	84.80 98.7%	72.09 99.0%	75.20 94.0%	57.11 93.2%	35.22 96.8%	62.44 93.3%	57.70 93.7%	95.3%
VisionZip 🔥 (2025a)	58.1 91.9%	65.6 96.9%	1671 91.9%	81.6 95.0%	72.3 99.3%	75.2 94.0%	58.5 95.4%	35.3 97.0%	61.4 91.8%	– –	94.8%
MMTok (Ours)	58.42 92.4%	65.72 97.1%	1763.39 97.0%	84.39 98.2%	72.98 100.2%	76.55 95.7%	58.40 95.3%	35.22 96.8%	63.39 94.8%	59.51 96.6%	**96.4%**

Table 17: **Performance Comparison on LLaVA-1.5-13B.** The vanilla number of visual tokens is 576. The first line of each method shows the raw benchmark accuracy, and the second line is the proportion relative to the upper limit. SEED-I represents SEED-IMG, SEED represents SEED-ALL. Following (Yang et al., 2025a), Avg. is based on SEED-I instead of SEED.

Method	GQA Acc. ↑	MMB Acc. ↑	MME P+C ↑	POPE F1 ↑	SQA Acc. ↑	VQA^{V2} Acc. ↑	VQA^{Text} Acc. ↑	MMMU Acc. ↑	SEED-I Acc. ↑	Avg. ↑
Avg. Images $\bar{n}$	4.90	4.12	4.53	4.90	3.85	4.98	4.98	4.07	4.72	
Avg. Tokens ($\bar{n} * 576$)	2822.4	2373.12	2609.28	2822.40	2217.60	2868.48	2868.48	2344.32	2718.72	
Upper Bound: 2880 (5×576) Tokens **(100%)**										
LLaVA-NeXT Vanilla 7B	64.2 100%	67.9 100%	1842 100%	86.4 100%	70.2 100%	80.1 100%	61.3 100%	35.1 100%	70.2 100%	100%
Upper: $5 \times 128 = 640$	627	527	580	627	493	638	638	521	604	↓ **77.8%**
SparseVLM (2024)	60.3 93.9%	65.7 96.8%	1772 96.2%	– –	67.7 96.4%	77.1 96.3%	57.8 94.3%	34.6 98.6%	– –	-
VisionZip (2025a)	61.3 95.5%	66.3 97.6%	1787 97.0%	86.3 99.9%	68.1 97.0%	79.1 98.8%	60.2 98.2%	34.7 98.9%	66.7 95.0%	97.5%
DivPrune (2025)	61.58 95.9%	65.38 96.3%	1773.04 96.3%	85.51 99.0%	67.82 96.6%	78.94 98.6%	55.41 90.4%	36.89 105.1%	67.56 96.2%	97.1%
VisionZip 🔥 (2025a)	62.4 97.2%	65.9 97.1%	1778 96.5%	87.6 101.4%	67.9 96.7%	79.9 99.8%	60.8 99.2%	37.2 106.0%	67.8 96.6%	98.9%
MMTok (Ours)	62.27 97.0%	65.29 96.2%	1829.28 99.3%	86.74 100.4%	68.47 97.5%	79.31 99.0%	58.97 96.2%	37.22 106.0%	67.74 96.5%	**98.7%**
Upper: $5 \times 64 = 320$	314	264	290	314	246	319	319	261	302	↓ **88.9%**
SparseVLM (2024)	57.7 89.9%	64.3 94.7%	1694 92.0%	– –	67.3 95.9%	73.4 91.6%	55.9 91.2%	34.4 98.0%	– –	-
VisionZip (2025a)	59.3 92.4%	63.1 92.9%	1702 92.4%	82.1 95.0%	67.3 95.9%	76.2 95.1%	58.9 96.1%	35.3 100.6%	63.4 90.3%	94.5%
DivPrune (2025)	59.63 92.9%	63.66 93.7%	1731.04 94.0%	83.47 96.6%	67.82 96.6%	76.64 95.7%	53.84 87.8%	37.11 105.7%	65.35 93.1%	95.1%
VisionZip 🔥 (2025a)	61.0 95.0%	64.4 94.8%	1770 96.1%	86.2 99.8%	67.5 96.2%	78.4 97.9%	59.3 96.7%	38.0 108.3%	65.9 93.9%	97.6%
MMTok (Ours)	60.96 95.0%	64.35 94.8%	1799.33 97.7%	85.76 99.3%	67.33 95.9%	77.68 97.0%	56.93 92.9%	38.00 108.3%	66.29 94.4%	**97.3%**
Upper: $5 \times 32 = 160$	157	132	145	157	123	159	159	130	151	↓ **94.4%**
SparseVLM (2024)	51.2 79.8%	63.1 92.9%	1542 83.7%	– –	67.5 96.2%	66.3 82.8%	46.4 75.7%	32.8 93.4%	– –	-
VisionZip (2025a)	55.5 86.4%	60.1 88.5%	1630 88.5%	74.8 86.6%	68.3 97.3%	71.4 89.1%	56.2 91.7%	36.1 102.8%	58.3 83.0%	90.4%
DivPrune (2025)	57.79 90.0%	62.29 91.7%	1658.25 90.0%	79.36 91.9%	68.02 96.9%	73.92 92.3%	52.42 85.5%	36.44 103.8%	62.54 89.1%	92.4%
VisionZip 🔥 (2025a)	58.2 90.7%	63.9 94.1%	1699 92.2%	83.4 96.5%	67.5 96.2%	75.6 94.4%	57.3 93.5%	37.7 107.4%	62.9 89.6%	95.0%
MMTok (Ours)	60.05 93.5%	62.97 92.7%	1715.54 93.1%	83.87 97.1%	67.97 96.8%	75.62 94.4%	54.17 88.4%	37.89 107.9%	64.54 91.9%	**95.1%**

Table 18: **Performance Comparison on LLaVA-NeXT-7B.** The vanilla number of visual tokens varies by dataset due to dynamic image processing (max 2880 for 5 images). '-' means performance not available in the original paper.

Method	GQA Acc. ↑	MMB Acc. ↑	MME P+C ↑	POPE F1 ↑	SQA Acc. ↑	VQA^{V2} Acc. ↑	VQA^{Text} Acc. ↑	MMMU Acc. ↑	SEED-I Acc. ↑	Avg. ↑
Avg. Images $\bar{n}$	4.90	4.12	4.53	4.90	3.85	4.98	4.98	4.07	4.72	
Avg. Tokens ($\bar{n} * 576$)	2822.4	2373.12	2609.28	2822.40	2217.60	2868.48	2868.48	2344.32	2718.72	
Upper Bound: 2880 (5 × 576) Tokens **(100%)**										
LLaVA-NeXT Vanilla 13B	65.4 100%	70.0 100%	1901 100%	86.2 100%	73.5 100%	81.8 100%	64.3 100%	36.2 100%	71.9 100%	100%
Upper: 5 × 128 = 640	627	527	580	627	493	638	638	521	604	↓ **77.8%**
VisionZip (2025a)	63.0 96.3%	68.6 98.0%	1871 98.4%	85.7 99.4%	71.2 96.9%	79.7 97.4%	62.2 96.7%	36.4 100.5%	68.8 95.7%	97.7%
DivPrune (2025)	62.82 96.1%	66.84 95.5%	1832.76 96.4%	86.17 99.9%	71.84 97.7%	79.87 97.6%	57.54 89.5%	37.78 104.4%	69.38 96.5%	97.1%
VisionZip 🔥 (2025a)	63.7 97.4%	66.6 95.1%	1829 96.2%	86.3 100.1%	73.2 99.6%	81.2 99.3%	64.4 100.2%	38.1 105.2%	69.2 96.2%	98.8%
MMTok (Ours)	63.71 97.4%	67.44 96.3%	1874.63 98.6%	86.72 100.6%	72.29 98.4%	80.55 98.5%	61.06 95.0%	37.11 102.5%	69.61 96.8%	**98.2%**
Upper: 5 × 64 = 320	314	264	290	314	246	319	319	261	302	↓ **88.9%**
VisionZip (2025a)	60.7 92.8%	67.2 96.0%	1805 95.0%	82.0 95.1%	70.3 95.6%	76.8 93.9%	60.9 94.7%	35.6 98.3%	65.2 90.7%	94.7%
DivPrune (2025)	61.03 93.3%	65.46 93.5%	1802.79 94.8%	84.86 98.4%	71.39 97.1%	77.6 94.9%	55.75 86.7%	36.00 99.4%	66.75 92.8%	94.5%
VisionZip 🔥 (2025a)	62.5 95.6%	66.9 95.6%	1861 97.9%	85.7 99.4%	72.7 98.9%	80.0 97.8%	63.2 98.3%	36.9 101.9%	67.9 94.4%	97.8%
MMTok (Ours)	62.95 96.3%	65.55 93.6%	1840.10 96.8%	85.88 99.6%	72.38 98.5%	78.79 96.3%	58.88 91.6%	36.33 100.4%	67.81 94.3%	**96.4%**
Upper: 5 × 32 = 160	157	132	145	157	123	159	159	130	151	↓ **94.4%**
VisionZip (2025a)	57.8 88.4%	64.9 92.7%	1739 91.5%	76.6 88.9%	69.3 94.3%	72.4 88.5%	58.4 90.8%	37.0 102.2%	61.1 85.0%	91.4%
DivPrune (2025)	59.34 90.7%	64.78 92.5%	1699.83 89.4%	82.16 95.3%	70.55 96.0%	74.72 91.3%	54.65 85.0%	35.89 99.1%	63.80 88.7%	92.0%
VisionZip 🔥 (2025a)	59.7 91.3%	65.3 93.3%	1766 92.9%	84.0 97.4%	72.0 98.0%	77.6 94.9%	60.8 94.6%	36.0 99.4%	64.4 89.6%	94.6%
MMTok (Ours)	61.94 94.7%	65.89 94.1%	1811.35 95.3%	85.11 98.7%	72.43 98.5%	76.8 93.9%	55.91 87.0%	37.11 102.5%	65.45 91.0%	**95.1%**

Table 19: **Performance Comparison on LLaVA-NeXT-13B.** The vanilla upper number of visual tokens is 2880. SEED-I represents SEED-IMG.

Method	GQA Acc. ↑	MMB Acc. ↑	MME P+C ↑	POPE F1 ↑	VQA^{Text} Acc. ↑	SQA Acc. ↑	OCRBench Acc. ↑	Avg.† ↑
Dynamic Resolution (MinPix = 256 × 28 × 28, MaxPix = 2048 × 28 × 28), Upper Bound **(100%)**								
Avg. Tokens $\bar{T}$	358.5	276.9	867.6	359.6	976.5	323.0	652.8	
Qwen-2.5-VL-7B	60.48	83.25	2327	86.16	77.72	87.46	83.80	100%
Dynamic Res.	100%	100%	100%	100%	100%	100%	100%	
Fixed Resolution (MinPix = MaxPix = 2048 × 28 × 28), Upper Bound **(100%)**								
Qwen-2.5-VL-7B	58.59	83.59	2339	86.09	76.64	86.91	76.60	99.3%
Fixed Res.	96.9%	100.4%	100.5%	99.9%	98.6%	99.4%	91.4%	
Retain 20% $\bar{T}$	71.7	55.4	173.5	71.9	195.3	64.6	130.6	**↓ 80%**
VisionZip (2025a)	56.80	80.33	2174	83.38	70.43	84.23	59.50	94.2%
	93.9%	96.5%	93.4%	96.8%	90.6%	96.3%	71.0%	
DivPrune (2025)	56.70	76.98	2163	80.59	65.86	80.91	48.10	91.5%
	93.8%	92.5%	93.0%	93.5%	84.7%	92.5%	57.4%	
MMTok (Ours)	58.09	79.30	2217	82.38	70.49	81.61	59.60	**94.6%**
	96.0%	95.3%	95.3%	95.7%	90.7%	93.3%	71.1%	
Retain 10% $\bar{T}$	35.9	27.7	86.8	36.0	97.7	32.3	65.3	**↓ 90%**
VisionZip (2025a)	52.47	75.60	2003	78.90	63.78	82.30	36.90	87.5%
	86.8%	90.8%	86.1%	91.6%	82.1%	94.1%	44.0%	
DivPrune (2025)	53.43	72.85	1957	74.99	59.59	79.57	37.30	84.7%
	88.3%	87.5%	84.1%	87.0%	76.7%	91.0%	44.5%	
MMTok (Ours)	55.09	74.74	2051	78.75	63.90	80.47	43.60	**88.5%**
	91.1%	89.8%	88.1%	91.4%	82.2%	92.0%	52.1%	
Retain 5% $\bar{T}$	17.9	13.8	43.4	18.0	48.8	16.2	32.6	**↓ 95%**
VisionZip (2025a)	46.28	67.53	1677	66.38	54.49	79.57	19.70	75.4%
	76.5%	81.1%	72.1%	77.1%	70.1%	91.0%	23.5%	
DivPrune (2025)	49.01	65.89	1739	68.45	52.02	77.05	24.90	76.3%
	81.0%	79.1%	74.7%	79.4%	66.9%	88.1%	29.7%	
MMTok (Ours)	50.66	65.89	1796	71.35	55.95	77.19	30.70	**79.0%**
	83.8%	79.2%	77.2%	82.8%	72.0%	88.2%	36.6%	
0 Token **↓ 100%**								
Qwen-2.5-VL 7B	31.84	20.10	935	0.00*	38.93	71.10	1.80	33.8%
Text-Only	54.3%	24.0%	40.0%	0.0%*	50.8%	88.6%	2.1%	

Table 20: **Performance Comparison on Qwen-2.5-VL-7B-Instruct.** Avg.† is the average performance over the 5 datasets: GQA, MMB, MME, POPE, and VQA^{Text}. The first line of each method shows the raw benchmark accuracy, and the second line is the proportion relative to the upper limit. *Qwen-2.5-VL outputs `"No"` for all POPE questions when no visual tokens are provided, resulting in 0% F1 score.

Method	GQA Acc. ↑	MMB Acc. ↑	MME P+C ↑	POPE F1 ↑	SQA Acc. ↑	VQA^{Text} Acc. ↑	MMMU Acc. ↑	SEED-I* Acc. ↑	Avg@8 ↑	Avg@5 ↑	≥90% /8 ↑	≥80% /8 ↑
Vanilla Baseline (576 tokens)												
LLaVA-1.5-7B	61.9	64.7	1862	85.9	69.5	58.2	36.3	66.14	100.0%	100.0%	8/8	8/8
90% Threshold	55.71	58.23	1675.80	77.31	62.55	52.38	32.67	59.53	90.0%	90.0%	–	–
80% Threshold	49.52	51.76	1489.60	68.72	55.60	46.56	29.04	52.91	80.0%	80.0%	–	–
64 Tokens												
VisionZip	55.1	60.1	1690	77.0	69.0	55.5	36.2	57.84	93.0%	90.0%	5/8	8/8
DivPrune	57.78	59.28	1674.40	85.56	68.07	54.69	35.56	60.21	94.4%	93.1%	7/8	8/8
MMTok	58.29	61.17	1715.33	85.77	69.16	56.01	36.11	61.29	96.1%	94.7%	8/8	8/8
32 Tokens												
VisionZip	51.78	57.22	1580.43	68.88	68.77	53.23	35.11	53.28	88.1%	83.5%	3/8	8/8
DivPrune	55.11	58.93	1600	82.06	68.62	53.20	35.33	57.08	91.9%	89.6%	5/8	8/8
MMTok	55.95	58.59	1624.72	82.95	68.86	53.70	35.33	59.81	93.0%	91.0%	7/8	8/8
16 Tokens												
VisionZip	46.72	45.70	1326.89	51.84	67.67	49.74	35.00	46.66	78.4%	69.7%	2/8	3/8
DivPrune	51.10	53.09	1518	69.56	69.41	50.01	35.44	52.72	86.3%	81.4%	2/8	7/8
MMTok	53.31	54.30	1550.65	79.79	68.82	50.04	34.22	56.67	88.9%	86.4%	3/8	8/8
8 Tokens												
VisionZip	39.47	24.40	1069.94	23.66	64.30	44.62	33.67	38.46	63.3%	48.9%	2/8	2/8
DivPrune	46.09	43.13	1294	52.10	67.92	45.21	34.00	46.68	76.4%	68.4%	2/8	2/8
MMTok	49.06	49.06	1355.31	78.46	66.83	45.71	34.11	52.74	83.5%	79.8%	3/8	3/8
4 Tokens												
VisionZip	36.57	18.30	923.57	24.48	63.56	40.82	33.78	35.34	59.2%	43.8%	2/8	2/8
DivPrune	40.67	28.61	1134	33.33	65.20	42.54	33.33	40.99	66.3%	54.3%	2/8	2/8
MMTok	43.93	36.94	1290.31	74.84	65.64	43.52	34.00	48.10	77.5%	71.4%	2/8	3/8
2 Tokens												
VisionZip	35.94	16.84	890.28	26.48	63.31	39.55	33.78	34.62	58.4%	43.0%	2/8	2/8
DivPrune	38.58	21.48	991	37.60	64.60	42.16	33.44	38.43	63.5%	50.1%	2/8	2/8
MMTok	40.58	25.69	1122.42	68.95	64.90	42.42	32.67	42.89	70.9%	62.1%	2/8	3/8
0 Tokens												
Baseline	37.65	19.33	970.89	44.64	63.51	41.66	33.33	37.03	63.2%	50.2%	2/8	2/8

Table 21: **Extended Performance Comparison with Extremely Less Token Budgets on LLaVA-1.5-7B.** *SEED-I indicts SEEDBench-Image. Avg@8 is across all 8 datasets, while Avg@5 is on 5 High-IC datasets.

Method	GQA Acc. ↑	MMB Acc. ↑	MME P+C ↑	POPE F1 ↑	SQA Acc. ↑	VQA^{Text} Acc. ↑	MMMU Acc. ↑	SEED-I Acc. ↑	Avg@8 ↑	Avg@6 ↑	≥90% /8 ↑	≥80% /8 ↑
Vanilla Baseline (Upper 2880 tokens)												
LLaVA-NeXT-7B	64.2	67.9	1842	86.4	70.2	61.3	35.1	70.2	100.0%	100.0%	8/8	8/8
90% Threshold	57.78	61.11	1657.80	77.76	63.18	55.17	31.59	63.18	90.0%	90.0%	–	–
80% Threshold	51.36	54.32	1473.60	69.12	56.16	49.04	28.08	56.16	80.0%	80.0%	–	–
Upper 32×5 Tokens (160 Tokens) 5.6%												
VisionZip	55.5	60.1	1630	74.8	68.3	56.2	36.1	58.3	90.6%	87.5%	3/8	8/8
DivPrune	57.79	62.29	1658	79.36	68.02	52.42	36.44	62.54	92.4%	89.7%	6/8	8/8
MMTok	60.05	62.97	1716	83.87	67.97	54.17	37.89	64.54	95.2%	92.8%	7/8	8/8
Upper 16×5 Tokens (80 Tokens) 2.8%												
VisionZip	50.80	50.69	1431	61.82	66.93	51.65	34.44	51.77	81.8%	76.8%	2/8	3/8
DivPrune	55.73	59.97	1575	74.74	66.83	50.35	36.56	59.48	89.2%	85.7%	2/8	8/8
MMTok	58.23	62.54	1681	81.89	67.13	49.56	36.11	61.86	92.0%	89.6%	6/8	8/8
Upper 8×5 Tokens (40 Tokens) 1.4%												
VisionZip	41.87	28.35	999	21.22	64.25	42.85	31.44	41.93	62.1%	52.6%	1/8	2/8
DivPrune	52.87	55.76	1462	67.49	66.78	48.02	33.44	55.40	83.7%	79.9%	2/8	4/8
MMTok	54.52	59.88	1555	81.84	67.73	45.77	35.00	59.28	88.4%	85.2%	3/8	7/8
Upper 4×5 Tokens (20 Tokens) 0.7%												
VisionZip	36.56	18.38	814	0.40	63.56	35.36	31.56	34.98	52.1%	39.4%	1/8	2/8
DivPrune	49.57	48.54	1324	52.14	65.94	44.06	31.78	51.25	76.3%	71.0%	2/8	2/8
MMTok	49.60	51.20	1457	82.41	66.88	42.33	33.67	55.34	83.3%	79.2%	3/8	3/8
Upper 2×5 Tokens (10 Tokens) 0.3%												
VisionZip	36.17	17.96	823	0.80	62.91	32.84	30.56	34.31	50.9%	38.5%	0/8	2/8
DivPrune	45.19	37.11	1134	25.48	65.25	40.33	33.22	45.54	66.8%	57.8%	2/8	2/8
MMTok	45.72	38.75	1283	79.62	65.64	39.77	33.78	49.73	76.9%	71.0%	3/8	3/8
0 Tokens												
Baseline	38.23	17.87	867	25.84	64.60	37.77	31.56	37.43	57.5%	46.3%	1/8	2/8

Table 22: **Extended Performance Comparison with Extremely Less Token Budgets on LLaVA-NeXT-7B.** Avg@8 is across all 8 datasets, while Avg@6 is across 6 High-IC datasets. The "×5" notation indicates maximum sampling to 5 images. Average percentages are calculated relative to the vanilla baseline for each metric.